Geomechanics and Engineering, *Vol. 40, No. 1 (2025) 59-68*
https://doi.org/10.12989/gae.2025.40.1.059

Risk assessment of floor water inrush using random forest, VIKOR, and GIS: A case study

Mengke Han[1], Weitao Liu*[1,2], Jiyuan Zhao[1], Yanhui Du[1] and Liqiu Zhang[1]

[1]*College of Safety and Environmental Engineering, Shandong University of Science and Technology, Qingdao, 266590, China*
[2]*College of Energy and Mining Engineering, Shandong University of Science and Technology, Qingdao, 266590, China*

(*Received April 15, 2024, Revised December 3, 2024, Accepted December 17, 2024*)

Abstract. As mining depth continues to increase, coal mines face increasingly complex water inrush conditions and varying risk factors, making the assessment of floor water inrush (FWI) risk more challenging. To more accurately evaluate the risk of FWI, this study proposes a composite evaluation model integrating Random Forest (RF), the VIKOR method, and Geographic Information System (GIS). Taking the Yangcheng Coal Mine in North China as the study area, an evaluation index system for FWI risk is established, consisting of six key factors: fault fractal dimension (C1), seam dip angle (C2), mining depth (C3), key-strata thickness (C4), water pressure (C5), and dip length of the working face (C6). The RF algorithm is used to mine the data features, ensuring a more scientific and reasonable calculation of the weights. The results show the following weights: C1 = 0.108, C2 = 0.092, C3 = 0.168, C4 = 0.171, C5 = 0.368, and C6 = 0.093. GIS technology is employed to collect quantitative data of six key factors affecting FWI at 1314 grid center points in the mining area. The VIKOR method is then applied to process the data, obtaining a risk ranking for each point, with higher-risk points ranked first. The evaluation results are visually presented in GIS with a color gradient, transitioning from green to red, indicating increasing risks. Actual water outflow locations are found within the red zones, validating the effectiveness of the model. This FWI risk assessment method provides new insights and practical references for the prevention and control of water-related hazards in coal mining.

Keywords: evaluation; floor water inrush; geographic information system; random forest; VIKOR method

1. Introduction

In China, as the depth of mine mining increases, the incidence of various engineering disasters and accidents increases significantly, among which coal seam floor water inrush (FWI) disasters are prominent (Cao *et al*. 2022, Gu *et al*. 2020). FWI refers to a phenomenon in which water in a confined aquifer suddenly flows into the mining space through the water-isolating rock layer between the mining coal seam and the confined aquifer (Liu *et al*. 2023, Cao *et al*. 2021, Zhang *et al*. 2015). The complex geological environment of deep mines further increases the difficulty of predicting FWI, resulting in frequent water inrush accidents and posing a serious threat to the social economy and people's life safety (Wagner 2019). Therefore, studying the risk of FWI and carrying out effective assessment are of great significance to ensuring safe production in coal mines (Huang *et al*. 2023).

The assessment of the risk of FWI is a complex multidisciplinary task that requires the comprehensive application of knowledge from multiple fields such as coal mine geology, structural geology, hydrogeology, geomechanics, and mathematical geology (Fan *et al*. 2024). In 1944, Hungarian scientist REIBIEZC first proposed the concept of relative aquiclude of the floor and established a theoretical framework for the relationship between water pressure, thickness of the aquiclude, and FWI (Meng *et al*. 2012). In 1948, Soviet scientist Slisalif proposed the concept of a fixed beam based on the theory of statics, simulating the floor as a fixed beam at both ends under uniform load, and combined with the rock strength theory to analyze its deformation and failure mechanism, and proposed a theoretical formula for predicting FWI. In 1964, Chinese scholars proposed an FWI coefficient method based on the FWI mechanism in combination with domestic mining area data (Shi 2012). Although this method has certain limitations, it is still one of the most commonly used FWI evaluation technologies in China. In the 21st century, Wu *et al*. (2013, 2017) proposed a comprehensive prevention and control index system for FWI, introduced the vulnerability index method, and used GIS technology to classify the risk of FWI, which greatly improved the accuracy of the assessment. In addition, many mathematical methods have been developed and applied to the refined assessment of FWI risk, such as variable weight theory (Wu *et al*. 2024), attribute mathematical theory (Xu *et al*. 2021), the TOPSIS method (Zhang *et al*. 2021), the cloud model (Li *et al*. 2023), etc. These methods have shown good application effects in a variety of coal mine environments and provided valuable experience for mine water hazard prevention and control. However, these traditional methods still have some shortcomings: Some evaluation methods rely on subjective weight calculation and lack objectivity; some methods only consider a few indicators and are difficult to reflect the multiple complexities of FWI; the

*Corresponding author, Professor
E-mail: skdlwt@126.com

ISSN: 2005-307X (Print), 2092-6219 (Online)

multi-factor effect of FWI and the inconsistency of indicator dimensions also pose great challenges to risk assessment technology (He *et al*. 2021).

In response to the above problems, this paper proposes a new scheme for assessing the risk of FWI based on RF-VIKOR-GIS. The VIKOR method is a multi-objective decision analysis tool that determines the ranking of the evaluation objects by calculating the distance between the evaluation object and the positive ideal solution and the negative ideal solution. It can achieve a trade-off between multi-dimensional indicators and thus handle complex decision-making problems. It is particularly suitable for the detailed assessment of the risk of FWI (Zhang *et al*. 2023). However, the VIKOR method is sensitive to the choice of weights, and unreasonable weights may lead to assessment bias. Therefore, the scientific nature of the weight calculation is crucial. Traditional subjective weight methods, such as the analytical hierarchy process (Kim *et al*. 2022), have the problem of insufficient subjectivity, while objective weight methods, such as the entropy weight method (Wei *et al*. 2020), also have certain limitations due to ignoring the conflicts between indicators. In addition, combined weight calculation methods such as linear weighting and multiplication weighting may lead to insufficient accuracy of the comprehensive weight due to uneven preference distribution. To solve the above problems, this paper combines the random forest (RF) algorithm with the VIKOR method, uses the RF algorithm to calculate the importance of the FWI evaluation index, and uses it as the weight input of VIKOR. By constructing multiple decision trees and integrating their results, RF can effectively identify the potential rules in the data, learn the relationship between evaluation indicators and FWI risks, and thus generate more scientific and reasonable data-driven weights. This method not only avoids the influence of human factors on weight setting but also improves the reliability and accuracy of the VIKOR method in risk assessment (Lai *et al*. 2018). On this basis, the spatial data of the mining area is analyzed in combination with geographic information system (GIS) technology. By quantitatively analyzing the factors affecting FWI at different grid center points, the RF-VIKOR method is used to rank the FWI risk of each grid point. Points with higher risk rankings indicate higher FWI danger. Finally, combined with the visualization function of GIS, the risk assessment results were intuitively presented in the form of a map, and the change in risks was displayed through a color gradient (from green to red). The FWI risk evaluation process in this paper is shown in Fig. 1. This comprehensive method not only improves the accuracy of the assessment but also provides an intuitive and effective decision support tool for mine management, helping managers to accurately identify high-risk areas and take targeted measures.

The new FWI risk assessment method based on RF-VIKOR-GIS proposed in this paper fully integrates the advantages of machine learning, decision analysis, and geographic information technology and can achieve efficient and accurate FWI risk prediction and assessment in complex mining environments, providing strong support for mine safety production and disaster prevention and control.

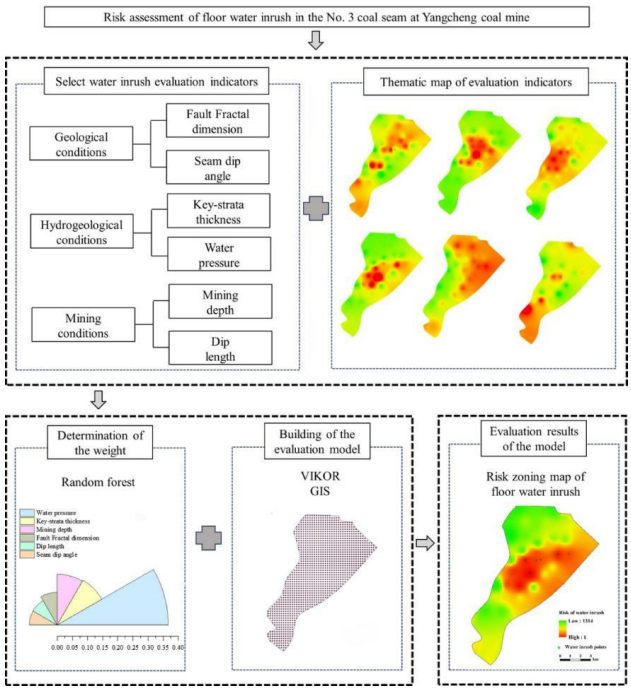

Fig. 1 FWI risk evaluation process

2. Methods

This study employs the RF algorithm to ascertain the weights of evaluation indicators. Integrate GIS technology to obtain relevant data for each evaluation indicator at the grid center point of the mining area. The VIKOR method is utilized for a comprehensive assessment of FWI risk at all points. The evaluation results, ordered by the risk of FWI, are presented visually using GIS.

2.1 Random Forest (RF)

2.1.1 RF principle

RF is proposed by Leo Breiman (2001). It is an ensemble learning method that builds a powerful classifier or regression model by integrating multiple weak learners (decision trees). This study focuses on the classification technology of RF (Sun *et al*. 2021). The construction process is: first, taking n training samples from the original training set with replacement through Bootstrap sampling to form a new training set. Subsequently, k decision tree models are constructed for each of the k samples to acquire k classification outcomes. Ultimately, each record is subjected to a voting process based on these k classification results. The category with the most votes is the final model prediction result (see Fig. 2). RF exhibits good robustness to high-dimensional data and data with noise and has strong resistance to over-fitting, which enhances its superiority in practical applications.

2.1.2 The principle of RF calculating the weight of each indicator

To evaluate the contribution of different features (this

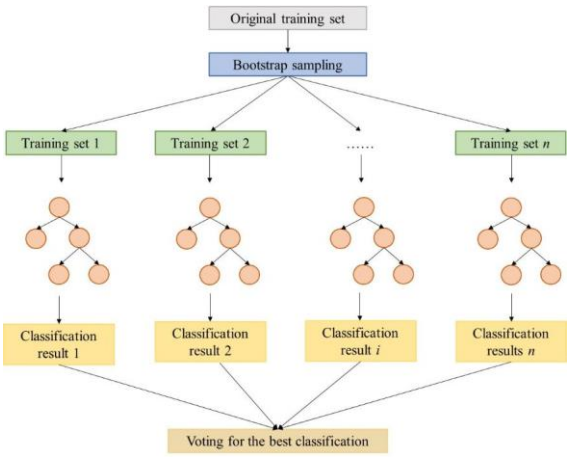

Fig. 2 RF decision process

study refers to the evaluation indicators) to the model performance, we adopted the feature weight calculation method based on the Gini index (Asaduzzaman *et al*. 2021). This method assesses the relative weight of each feature by gauging its impact on enhancing the performance of the RF model. Utilizing the RF algorithm to acquire the weight of the indicators, we can reduce the subjectivity of evaluation results.

(1) The Gini index. At each node of the decision tree, the Gini index is used to measure the impurity of that node. For the two-category problem of FWI or not, the Gini index is defined as follows

$$Gini(t)=1-\sum_{i=1}^{2}(p_i)^2 \tag{1}$$

where p_i represents the proportion of samples belonging to category i in node t.

(2) The Gini gain. For a node t, the Gini gain represents the degree to which the Gini index decreases after the node is split

$$GG=G(P)-\left(\frac{N_L}{N_t}\cdot G(L)+\frac{N_R}{N_t}\cdot G(R)\right) \tag{2}$$

Where GG: Gini gain; $G(P)$: Gini index of the parent node; NL: Number of samples in the left child node; NR: Number of samples in the right child node; $G(L)$: Gini index of the left child node; $G(R)$: Gini index of the right child node.

(3) Feature weight. To calculate feature weights, the Gini gain is calculated for each node of each decision tree, and the gains on the same feature are accumulated. Finally, for each feature, we average its Gini gain across all decision trees to obtain the feature weight.

$$FW=\frac{1}{N}\sum_{i=1}^{N} G G_i \tag{3}$$

Where FW: Feature weight; N: Total number of samples; GG_i represents the Gini gain in the i-th decision tree.

(4) Normalized feature weight.

$$NFW_i=\frac{FW_i}{\sum_{j=1}^{n} FW_j} \tag{4}$$

where NFW_i is the normalized feature weight of the i-th feature, and FW_i is the feature weight of the i-th feature. $\sum_{j=1}^{n} F W_j$ is the sum of all feature weights. The normalized feature weight is the weight of the indicator that need to be obtained.

2.2 VIKOR method

The VIKOR method is a MCDM technique proposed by Professor Opricovic (1998). It relies on the Lp metric aggregation function and calculates the compromise solution for each evaluation object (the grid center point in the study area) by determining the "positive ideal solution (f^+)" and the "negative ideal solution (f^-)." The core of this method is to attain a viable compromise solution that is closest to the f^+ and farthest from the f^- through mutual concessions between attributes, and then determine the quality of the evaluated object. Its most prominent feature lies in its compromise between maximizing "group benefit (S)" and minimizing "individual regret (R)," rendering this method more rational for addressing multi-attribute decision-making problems. The VIKOR method is mainly divided into five steps: determining weights, standardizing data, calculating ideal solutions, calculating S and R, and calculating and ranking benefit ratio (Q).

(1) Calculation of evaluation indicator weights. A variety of weighting methods can be used. Commonly used methods include the AHP, the CRITIC method, the combined weighting method, etc. This study uses the RF algorithm to calculate the weight of the indicators.

(2) Standardized data. Standardizing data is the process of converting data into a dimensionless form for ease of use. The data standardization formula for the VIKOR method is:

For positive indicators

$$r_{ij}=\frac{a_{ij}}{\sqrt{\sum_{i=1}^{m} a_{ij}^2}} \quad i=1,2,\cdots,m;j=1,2,\cdots,n \tag{5}$$

For negative indicators

$$r_{ij}=\frac{1/a_{ij}}{\sqrt{\sum_{i=1}^{m} (1/a_{ij})^2}} \quad i=1,2,\cdots,m;j=1,2,\cdots,n \tag{6}$$

Where, r_{ij} is the standardized data of the j-th evaluation indicator in the i-th evaluation object; a_{ij} is the original data of the j-th evaluation indicator in the i-th evaluation object.

(3) Calculate the ideal solution. The f^+ represents the optimal scenario where positive indicators are maximized and negative indicators are minimized, while the f^- denotes the optimal scenario where positive indicators are minimized, and negative indicators are maximized. In this study, it is stipulated that the increase of the positive indicators increases the risk of FWI, while the increase of the negative indicators weakens the FWI. The calculation formula for the ideal solution is as follows

$$f_j^+=1 \tag{7}$$

$$f_j^-=0 \tag{8}$$

Where, f_j^+ is the f^+ of the j-th indicator, and f_j^- is the f^- of the j-th indicator.

(4) Calculate the S and the R:

Taking the f^+ as a reference

$$S_i^+ = \sum_{j=1}^{n} \omega_j \frac{f_j^+ - r_{ij}}{f_j^+ - f_j^-} \quad i=1,2,\cdots,m; j=1,2,\cdots,n \tag{9}$$

$$R_i^+ = \mathrm{Max}_j\, \omega_j \frac{f_j^+ - r_{ij}}{f_j^+ - f_j^-} \quad i=1,2,\cdots,m; j=1,2,\cdots,n \tag{10}$$

Taking the f^- as a reference

$$S_i^- = \sum_{j=1}^{n} \omega_j \frac{r_{ij} - f_j^-}{f_j^+ - f_j^-} \quad i=1,2,\cdots,m; j=1,2,\cdots,n \tag{11}$$

$$R_i^- = \mathrm{Min}_j \frac{r_{ij} - f_j^-}{f_j^+ - f_j^-} \quad i=1,2,\cdots,m; j=1,2,\cdots,n \tag{12}$$

The S and R of the evaluation object

$$S_i = \frac{S_i^+}{S_i^-} \quad i=1,2,\cdots,m \tag{13}$$

$$R_i = \frac{R_i^+}{R_i^-} \quad i=1,2,\cdots,m \tag{14}$$

Where, S_i^+ and R_i^+ represent the S and R for the *i-th* evaluation object, with the f^+ as a reference. Similarly, S_i^- and R_i^- denote the S and R for the *i-th* evaluation object, with the f^- as the reference. Meanwhile, S_i and R_i stand for the S and R of the *i-th* evaluation object, respectively.

(5) Calculate Q and sort. We set the decision-making mechanism coefficient to 0.5, indicating a balanced approach that involves maximizing S and minimizing R simultaneously. The results of the Q are sorted in descending order. The smaller the Q value, the better the result, indicating a higher risk of FWI at the evaluation object (grid center point).

Taking the f^+ as a reference

$$Q_i = u\frac{S_i - S_{imin}}{S_{imax} - S_{imin}} + (1-u)\frac{R_i - R_{imin}}{R_{imax} - R_{imin}} \quad i=1,2,\cdots,m \tag{15}$$

$$S_{imax} = maxS_i,\ S_{imin} = minS_i,\ R_{imax} = maxR_i,\ R_{imin} = minR_i \tag{16}$$

Where, Q_i is the benefit ratio; u is the decision-making mechanism coefficient.

2.3 GIS technology

The RF-VIKOR model provides evaluation results at the point level but lacks spatial representation. To address this limitation, supplementary tools are essential for extending the obtained evaluation results. To fulfill this objective, the RF-VIKOR model was augmented with GIS technology for a more comprehensive assessment of FWI risk.

The integration application of the RF-VIKOR model and GIS for FWI risk evaluation includes the following four stages: (1) Thematic maps for each evaluation indicator are crafted utilizing the geological and hydrogeological data specific to the study area. And utilizing the robust spatial information analysis and processing capabilities of GIS, the values of the grid center point are extracted from the thematic map of each indicator. (2) Use the grid search method to select the RF hyperparameter value, conduct training based on the normalized data, and calculate the weight of each indicator. (3) Use the VIKOR method to comprehensively evaluate all points and obtain the Q of each point to rank the FWI risks at each point. (4) Finally, the FWI evaluation results are visually displayed in GIS in graphical form based on the sorting results.

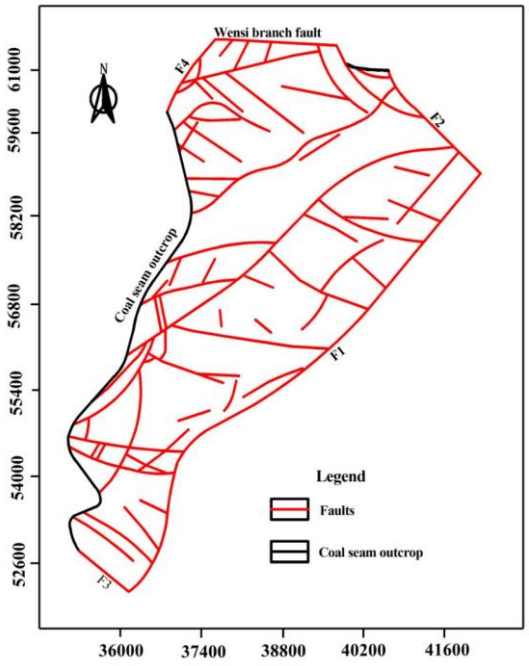

Fig. 3 The study area

3. Experiments

3.1 Engineering geology overview

Yangcheng Coal Mine, a North China-type coalfield, is the study area of this study (see Fig. 3). The wellfield boundaries of Yangcheng Coal Mine are: the eastern boundary originates from the F1 fault, and the western boundary ends at the Taiyuan Formation 17 coal seam outcrop; the southern boundary originates from the F3 fault; the northern boundary ends at the Wensi branch fault; and the northeast corner is the F2 fault.

3.1.1 Mining geological conditions

The Yangcheng Coal Mine represents a North China-type sedimentary coalfield characterized by a stratigraphic sequence comprising Ordovician, Carboniferous, Permian, and Quaternary layers, arranged from bottom to top. The strata exhibit a NE strike and SE dip, with dip angles ranging from 11° to 50°. The geological structure includes an extensive network of fault structures, totaling 124 faults, all of which are normal faults. Notably, there are no collapse columns or magmatic rock intrusions. Coal seam No. 3, extracted from the Shanxi Formation of the Lower Permian System, is a mineable coal seam across the entire region. It exhibits a thickness ranging from 4 m to 9.5 m, with an average coal thickness of 7.5 m, and dip angles ranging from 9° to 30°.

3.1.2 Hydrogeological conditions

In the context of coal seam No. 3 mining, the study area primarily encompasses three aquifers, arranged from top to bottom: the lower Quaternary gravel layer, the 3-coal roof and floor sandstone layer, and the middle Ordovician limestone. The Ordovician aquifer is the one posing a significant threat. It has a thickness ranging from 161.55 m to 175.00 m, with an average thickness of 165.00 m and a unit water inflow ranging from 0.275L/(s·m) to 0.490L/(s·m). This aquifer is characterized as a regional strong aquifer with uneven water content.

There are three aquitards situated between different aquifers, namely the Middle Zhongji Group aquitard in the Quaternary system, the Lower Shihexia Group mudstone and sandstone aquitard, and the Benxi Group aquitard. Among these, the Benxi Group aquitard is the one effectively impeding the Ordovician aquifer. Positioned beneath coal seam No. 3, it has a thickness ranging from 65.04m to 125.14m. The upper part comprises dolomitic limestone and thin-bedded limestone, while the lower part is composed of ferruginous mudstone, mudstone, and claystone. This aquitard exhibits relatively favorable hydraulic resistance properties.

3.2 Results and discussions

A risk assessment model was developed to evaluate the potential for FWI in karst aquifers, utilizing the RF-VIKOR approach along with GIS. The essential steps include: (1) Selection of evaluation indicators. (2) Computation of RF weights for the chosen indicators. (3) Application of the model, followed by the evaluation and verification of the obtained results.

3.2.1 Selection of evaluation indicators

An important part of evaluating FWI is building the evaluation indicator system. Hence, we consulted influencing factors identified in prior studies on FWI risk (Zhang and Li 2022, Meng *et al*. 2012, Lu *et al*. 2020, Wu *et al*. 2017, Zhang and Yang 2021). Taking into account geological, hydrogeological, and mining conditions, we selected six factors as evaluation indicators: fault fractal dimension (C1), seam dip angle (C2), mining depth (C3), key-strata thickness (C4), water pressure (C5), and dip length of the working face (C6). The impact of these indicators on FWI can be classified into two types: positive correlation and negative correlation. Notably, factors demonstrating a positive correlation with the risk of FWI encompass C1, C2, C3, C5, and C6. Conversely, the sole factor exhibiting a negative correlation is C4.

(1) Fault Fractal Dimension (C1): Faults can be characterized by factors such as distribution, intersection, and endpoints, which are difficult to quantify directly. The fractal dimension method, based on fractal theory, integrates these factors into a single parameter. The fault fractal dimension is calculated as $d=\lg N(s)/\lg s$, where $N(s)$ represents the number of fault traces within a grid, and s is the grid length. A higher fault fractal dimension indicates a more complex fault structure, which increases the risk of FWI (Wang *et al*. 2024).

(2) Seam Dip Angle (C2): The dip angle of the coal seam affects the distribution of stress and water pressure in the mining area (Song and Zhao 2024). A steeper seam dip increases the depth of floor failure, thereby elevating the risk of FWI.

(3) Mining Depth (C3): As mining depth increases, the mine pressure also increases, leading to a higher likelihood of floor fractures, which create channels for FWI (Li *et al*. 2022). This raises the risk of FWI, making mining depth a critical factor in assessing the potential for FWI.

(4) Key-Strata Thickness (C4): Key strata are high-strength layers within water-resistant strata that prevent water from flow the working face. As the thickness of the key strata decreases, the risk of FWI increases (Zhang and Li 2022, Ma *et al*. 2022).

(5) Water Pressure (C5): High groundwater pressure can cause the water-resistant strata to fracture, allowing water to flow into the mine and increase the likelihood of FWI (Zhang *et al*. 2024).

(6) Dip Length of the working face(C6): Dip length is the ratio of the working face length on the engineering plan to the cosine of the seam dip angle, serving as a measure of the mining space. Longer dip lengths result in higher stress concentrations around the mining face, leading to more severe failure of key strata and a greater risk of FWI (Lu *et al*. 2020).

Six single-factor thematic maps (see Fig. 4) were generated utilizing the geospatial information from mine drilling data, with the 33 sets of raw data referenced in Table 1 (Liu and Han 2023). Initially, the GIS grid interpolation method was applied to these 33 sets of data to generate thematic maps for each indicator, covering the entire mining area. The factor data at each location in the thematic map is stored in the attribute table of GIS. As shown in Fig. 4, for positively correlated variables, the mining area's central, eastern, and northeastern regions exhibit larger values for C3; the southern region shows larger values for C6, while in the central area, C1, C2, and C5 values are higher, indicating a greater risk of FWI. For the negatively correlated variable C4, the central region has smaller values, which also corresponds to higher FWI risk.

The grid center points shown in Fig. 5 were evenly distributed across the six thematic maps of the evaluation indicators, totaling 1314 points. The relevant data for the six factors at these 1314 points were retrieved from the attribute table of GIS.

3.2.2 Computation of RF weights for the chosen indicators

In RF, ensuring the model's effectiveness hinges on the careful selection of characteristic sample points that show significant differences in risk values. The principles for selecting sample points in this study are as follows: (1) Borehole points identified as having FWI risk are marked with a risk value of 1. (2) Borehole points without FWI risk are marked with a risk value of 0. Given the limited number of borehole data available in Table 1, there are only six borehole points with FWI risk. Therefore, in order to achieve a balanced representation of both FWI and non-FWI cases, six FWI borehole points and six non-FWI

Table 1 The raw data of borehole points

Number	Data related to each evaluation indicator						Water inrush or not?
	C1	C2(°)	C3(m)	C4(m)	C5(Mpa)	C6(m)	
1	0.706	10	706	56.33	0.3	175.51	No
2	0.733	10	680	56.05	0.3	250.24	No
3	0.756	12	929	30.29	0.5	200.25	No
4	0.879	12	915	33.12	0.5	200.65	No
5	0.793	12	243	65.00	0	98.58	No
6	0.808	10	726	37.29	0.5	182.15	No
7	0.796	10	750	34.77	0.5	192.84	No
8	0.875	10	740	40.00	0.5	192.68	No
9	0.884	15	570	32.84	0	143.56	No
10	0.927	15	887	45.56	1.2	197.55	No
11	0.752	20	374	33.01	0	170.26	No
12	0.884	20	670	38.56	2.3	198.02	No
13	0.927	10	925	45.66	3.6	159.53	Yes
14	0.740	10	956	35.50	2.3	209.38	Yes
15	0.915	20	547	10.50	3.4	275.34	Yes
16	0.656	9	262	20.00	0.3	150.02	No
17	0.714	20	760	28.60	2.1	183.92	Yes
18	0.712	20	872	32.00	0.6	180	No
19	0.756	10	392	10.00	3.3	200	No
20	0.743	15	871	58.89	1.1	108.94	No
21	1.062	20	390	12.81	2.5	120.5	No
22	0.971	20	529	12.37	3.7	200.1	No
23	0.680	12	901	33.42	0.3	91.47	No
24	0.695	9	267	38.80	0	189.82	No
25	0.695	9	252	25.00	0	189.82	No
26	0.717	11	409	27.00	1.3	190.05	No
27	0.979	20	769	15.00	4.2	275.42	Yes
28	0.718	25	519	18.63	5.2	200	Yes
29	0.791	11	431	34.57	1.3	300.63	No
30	0.614	13	699	36.60	1.2	175.47	No
31	0.911	10	350	35.00	0.2	347.55	No
32	0.831	10	671	48.80	0.5	220.05	No
33	0.870	10	746	64.00	1.2	250.13	No

borehole points were selected from Table 1 as sample points (see Table 2). This selection is based on the principle of uniform distribution. The risk value of each sample point, along with the corresponding data for each evaluation indicator, was used as the feature set for the RF model.

To assess the model's predictive power, the dataset was split into training and testing sets with a 7:3 ratio. The samples corresponding to the numbers 2, 4, 8, and 12 in Table 2 were designated as the testing set. Hyperparameter optimization was performed using the grid search method to identify the most suitable configuration. During this process, various combinations of hyperparameters, such as the number of estimators (n_estimators) and the maximum depth of the trees (max_depth), were tested, including 'n_estimators': [50, 100, 200], 'max_depth': [None, 3, 5, 7]. The results showed that the optimal configuration was achieved with n_estimators=50 and max_depth=None, meaning there was no limitation on the depth of the trees. This choice of hyperparameters allows the model to fully explore complex decision boundaries without overfitting, and the weight values of each indicator were obtained (see Table 3 and Fig. 6). Since the weights of C3, C4 and C5 are relatively large, their influence on FWI is relatively large. Combined with their single-factor thematic Figs. 4(c)-4(e), it can be inferred that the possibility of FWI is the greatest in the middle of the study area.

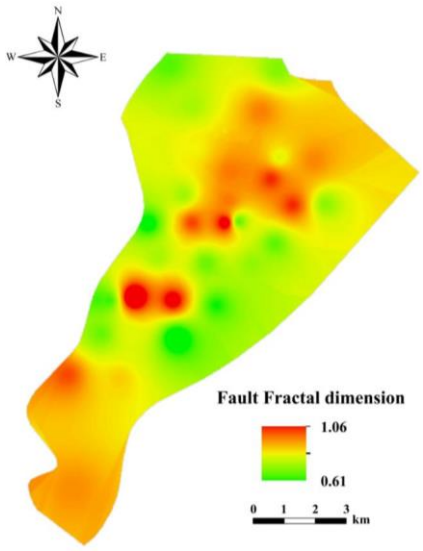

(a) C1

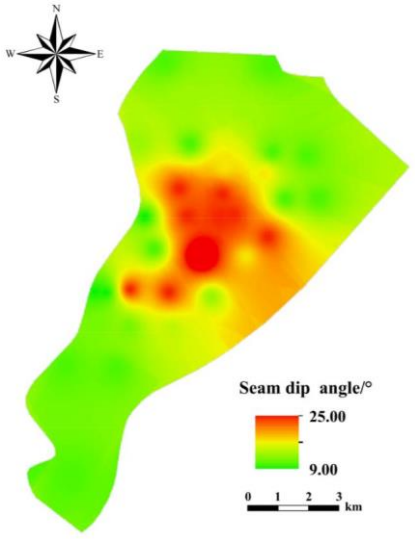

(b) C2

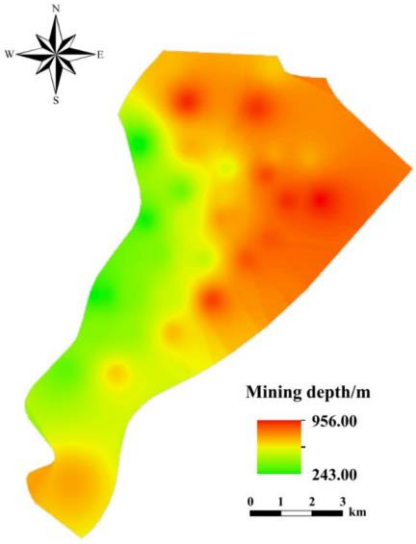

(c) C3

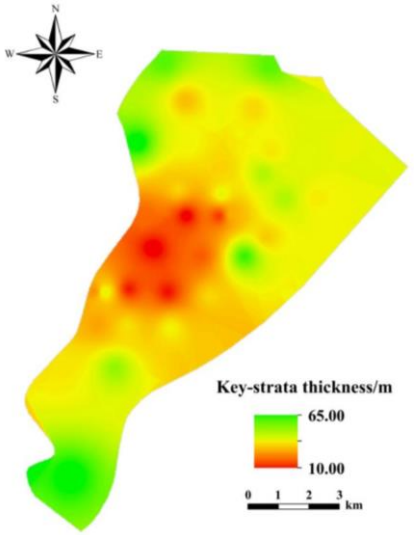

(d) C4

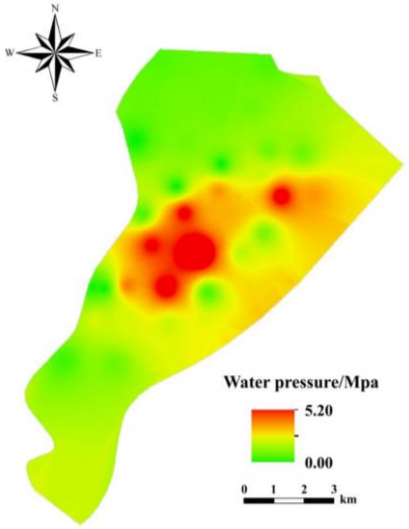

(e) C5

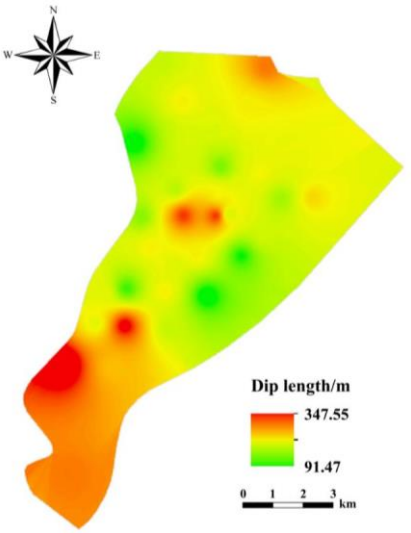

(f) C6

Fig. 4 Thematic maps of FWI evaluation indicators

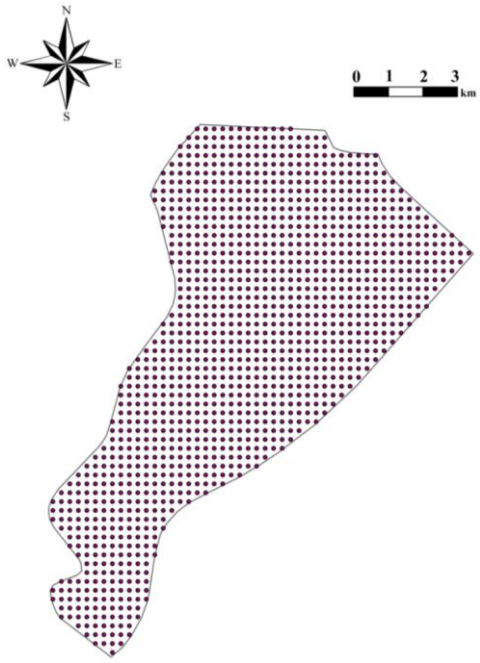

Fig. 5 Grid center point

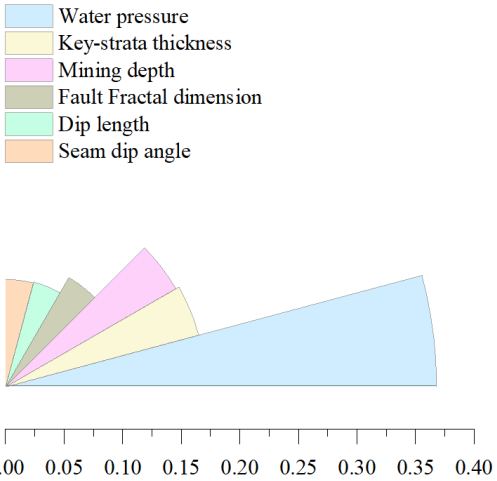

Fig. 6 RF weights

Table 2 Samples of FWI borehole points and non-FWI borehole points

Sample number	Data related to each evaluation indicator						Risk value
	C1	C2	C3	C4	C5	C6	
1	0.733	10	680	56.05	0.3	250.24	0
2	0.879	12	915	33.12	0.5	200.65	0
3	0.808	10	726	37.29	0.5	182.15	0
4	0.884	15	570	32.84	0	143.56	0
5	0.911	10	350	35.00	0.2	347.55	0
6	0.831	10	671	48.80	0.5	220.05	0
7	0.927	10	925	45.66	3.6	159.53	1
8	0.740	10	956	35.50	2.3	209.38	1
9	0.915	20	547	10.50	3.4	275.34	1
10	0.714	20	760	28.60	2.1	183.92	1
11	0.979	20	769	15.00	4.2	275.42	1
12	0.718	25	519	18.63	5.2	200	1

Table 3 RF weights

Evaluation indicator	C1	C2	C3	C4	C5	C6
RF weight	0.108	0.092	0.168	0.171	0.368	0.093

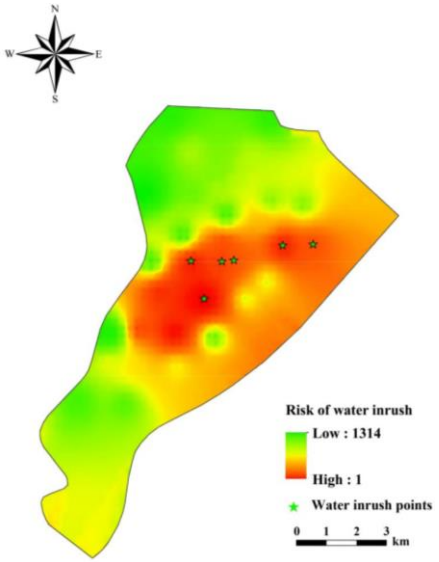

Fig. 7 Risk zoning of FWI

3.2.3 Application of the model, followed by the evaluation and verification of the obtained results

According to the above VIKOR Eqs. (5)-(16), combined with the RF weight of the indicator, the *S*, *R*, and *Q* values of each grid center point in the study area can be obtained (see Table 4). The grid center points in Table 4 are arranged according to the number, corresponding to the distribution order of the study area from south to north and from west to east in Fig. 5. That is, the point numbered 1 corresponds to the point at the southernmost and westernmost side of the study area in Fig. 5. The *Q* value is used to rank the FWI risk at each grid center point in the study area. The smaller the *Q* value, the higher the ranking. Since the ranking results directly obtained are in numerical form and lack spatial characteristics, GIS can be used to intuitively display the water inrush hazard in the study area. The ranking results are input into GIS, and the ranking results are visualized using the spatial interpolation function of GIS to generate a risk zoning map (see Fig. 7). Fig. 7 intuitively shows the spatial distribution of FWI risk in the study area.

The FWI risk in the central area of the study area is higher, which is consistent with the geological characteristics such as high mining depth, thin impermeable layer and high aquifer pressure area. These characteristics promote water influx through fractures, making the area particularly susceptible to FWI. In addition, there are six FWI points in the study area (see Table 2), all located in the central high-risk area, indicating that the assessment model is effectively consistent with the actual FWI occurrence. In addition, the risk areas predicted in this study are roughly the same as those in the papers that also predicted FWI in Yangcheng Coal Mine (Liu and Han 2023, Li and Sui 2021, Liu *et al*. 2021).

Table 4 *S*-value, *R*-value, *Q*-value and FWI ranking at the grid center points in the study area

Number	*S*	*R*	*Q*	FWI Ranking
1	0.6582	0.2819	0.6367	660
2	0.6571	0.2790	0.6307	637
3	0.6568	0.2789	0.6301	635
……	……	……	……	……
1312	0.6912	0.3365	0.7594	1185
1313	0.6959	0.3373	0.7644	1197
1314	0.7052	0.3388	0.7739	1210

4. Conclusions

This study developed an integrated evaluation model based on RF, VIKOR, and GIS to assess the risk of FWI in the No. 3 coal seam of the Yangcheng Coal Mine. The key findings are as follows:

• The VIKOR method was applied to rank the FWI risk at 1314 grid center points across the study area. GIS was used to generate a risk zoning map, which revealed a higher risk of FWI in the central part of the study area. The evaluation results were validated by comparing them with the actual FWI points, showing that all FWI points were situated in high-risk areas, confirming the model's predictive accuracy.

• The RF algorithm was employed to calculate the weights of six indicators: fault fractal dimension (C1: 0.108), seam dip angle (C2: 0.092), mining depth (C3: 0.168), key-strata thickness (C4: 0.171), water pressure (C5: 0.368), and dip length of the working face (C6: 0.093). This objective, data-driven approach ensured that the weight calculation was scientifically rigorous and minimized subjective biases in the evaluation process.

Acknowledgments

The research described in this paper was financially supported by the Natural Science Foundation of Shandong Province under Grant ZR2023ME002; and the National Natural Science Foundation of China under Grant 52304238.

References

Asaduzzaman, S., Ahmed, M.R., Rehana, H., Chakraborty, S., Islam, M.S. and Bhuiyan, T. (2021), "Machine learning to reveal an astute risk predictive framework for Gynecologic Cancer and its impact on women psychology: Bangladeshi perspective", *Bmc Bioinformatics*, **22**(1). https://doi.org/10.1186/s12859-021-04131-6.

Breiman, L. (2001), "Random forests", *Mach Learn*, **45**, 5-32.

Cao, M., Yin, S.X. and Xu, B. (2021), "Water inrush and failure characteristics of coal seam floor over a confined aquifer", *Energy Rep.*, **7**, 8298-8311. https://doi.org/10.1016/j.egyr.2021.10.007.

Cao, Z., Gu, Q., Huang, Z. and Fu, J. (2022), "Risk assessment of fault water inrush during deep mining", *Int. J. Min. Sci. Technol.*, **32**(2), 423-434. https://doi.org/10.1016/j.ijmst.2022.01.005.

Fan, H.D., Luo, F., Gao, S., Li, M., Lv, Z. and Sun, G. (2024), "Evolution law of mining-induced overburden stratum stress and fracture fields in inclined coal seam", *World J. Eng.*, **21**(3), 475-486. https://doi.org/10.1108/WJE-07-2023-0384.

Gu, Q.X., Huang, Z., Li, S.J., Zeng, W., Wu, Y. and Zhao, K. (2020), "An approach for water-inrush risk assessment of deep coal seam mining: a case study in Xinlongzhuang coal mine", *Environ. Sci. Pollut. Res.*, **27**, 43163-43176. https://doi.org/10.1007/s11356-020-10010-1.

He, J.H., Li, W.P., Qiao, W., Yang, Z. and Wang, Q.Q. (2021), "Risk assessment of water inrushes from bed separations in Cretaceous strata corresponding to different excavation lengths during mining in the Ordos Basin", *Geomatics Nat. Hazard. Risk*, **12**(1), 2300-2327. https://doi.org/10.1080/19475705.2021.1950220.

Huang, W.P., Sui, L., Wang, Y.M., Zhang, C.G., Jiang, D.H., Cai, X.W. and Yang, Z.X. (2023), "Study of the mining and aquifer interactions in complex geological conditions and its management", *Sci. Rep.*, **13**(1), 9462. https://doi.org/10.1038/s41598-023-38592-0.

Kim, H.K., Moon, J.S., An, J.W. and Michael, E.S. (2022), "Development of performance evaluation model for road and railway tunnels in use", *Geomech. Eng.*, **29**(3), 369-376. https://doi.org/10.12989/gae.2022.29.3.369.

Lai, C.G., Chen, X.H., Wang, Z.L., Xu, C.Y. and Yang, B. (2018), "Rainfall-induced landslide susceptibility assessment using random forest weight at basin scale", *Hydrol. Res.*, **49**(5), 1363-1378. https://doi.org/10.2166/nh.2017.044.

Li, C.Y., Zuo, J.P., Xing, S.K., Du, W.S. and Chuai, X.Y. (2022), "Failure behavior and dynamic monitoring of floor crack structures under high confined water pressure in deep coal mining: A case study of Hebei, China", *Eng. Fail. Anal.*, **139**, 106460. https://doi.org/10.1016/j.engfailanal.2022.106460.

Li, Q. and Sui, W.H. (2021), "Risk evaluation of mine-water inrush based on principal component logistic regression analysis and an improved analytic hierarchy process", *Hydrogeol. J.*, **29**(3), 1299-1311. https://doi.org/10.1007/s10040-021-02305-3.

Li, Q., Sui, W.H. and Sun, B.T. (2023), "Assessment of water inrush risk based comprehensive cloud model: a case study in a lead zinc mine, China", *Carbonates Evaporites*, **38**(1), 7. https://doi.org/10.1007/s13146-022-00758-7.

Liu, R., Zhi, G.J., Yang, S.L. and Xu, X.W. (2023), "Investigation on Mining-Induced Floor Water Inrush from Column and Its Control Based on Microseismic Monitoring", *Adv. Civ. Eng.*, **2023**(1), 3754079. https://doi.org/10.1155/2023/3754079.

Liu, W.T. and Han, M.K. (2023), "A practical method for floor water inrush prediction using a hybrid artificial intelligence model and GIS", *Mine Water Environ.*, **42**(2), 220-229. https://doi.org/10.1007/s10230-023-00919-w.

Liu, W.T., Han, M.K., Meng, X.X. and Qin, Y.Y. (2021), "Mine water inrush risk assessment evaluation based on the GIS and combination weight-cloud model: A case study", *ACS Omega*, **6**(48), 32671-32681. https://doi.org/10.1021/acsomega.1c04823.

Lu, Y., Bai, L.Y., Chen, J.T., Tong, W.X. and Jiang, Z. (2020), "Development and application of a floor failure depth prediction system based on the WEKA platform", *Geomech. Eng.*, **23**(1), 51-59. https://doi.org/10.12989/gae.2020.23.1.051.

Ma, K., Yang, T.H., Zhao, Y., Hou, X.G., Liu, Y.L., Hou, J.X., Zheng, W.X. and Ye, Q. (2022), "Mechanical model for analyzing the water-resisting key stratum to evaluate water inrush from goaf in roof", *Geomech. Eng.*, **28**(3), 299-311. https://doi.org/10.12989/gae.2022.28.3.299.

Meng, Z.P., Li, G.Q. and Xie, X.T. (2012), "A geological assessment method of floor water inrush risk and its

application", *Eng. Geol.*, **143**, 51-60. https://doi.org/10.1016/j.enggeo.2012.06.004.
Opricovic, S. (1998), "Multicriteria optimization of civil engineering systems", Ph.D. Dissertation, University of Belgrade, Belgrade.
Shi, L. (2012), "Analysis of the origin of water inrush coefficient and its applicability", *J. Shandong Univ. Sci. Technol. (Nat. Sci.)*, **31**(6), 6-9.
Song, W.C. and Zhao, C.B. (2024), "Influence analysis of strata dip on the failure characteristics and groundwater outburst risk of coal seam floor", *Environ. Earth Sci.*, **83**(16), 488. https://doi.org/10.1007/s12665-024-11018-3.
Sun, Y.T., Li, G.C., Zhang, J.F. and Huang, J.D. (2021), "Rockburst intensity evaluation by a novel systematic and evolved approach: machine learning booster and application", *Bull. Eng. Geol. Environ.*, **80**(11), 8385-8395. https://doi.org/10.1007/s10064-021-02460-7.
Wagner, H. (2019), "Deep mining: a rock engineering challenge", *Rock Mech. Rock Eng.*, **52**, 1417-1446. https://doi.org/10.1007/s00603-019-01719-8.
Wang, D.D., Sui, W.H. and Ji, Z.Q. (2024), "Fault complexity degree in a coal mine and the implications for risk assessment of floor water inrush", *Geomatics Nat. Hazards Risk*, **15**(1), 2293464. https://doi.org/10.1080/19475705.2023.2293464.
Wei, J.C., Zhao, Z.C., Xie, D.L., Yu, G. and Wu, X. (2020), "Water abundance evaluation of sandstone aquifer based on lithologic and structural characteristics", *J. Shandong Univ. Sci. Technol. (Nat. Sci.)*, **39**, 13-23.
Wu, F.Z., Du, J.M., Sun, F., Chen, G., Jiang, F. and Zhu, Z. (2024), "Multi-method coal seam floor water inrush risk evaluation based on variable weight theory", *Energy Explor. Exploit.*, https://doi.org/10.1177/01445987241295833.
Wu, Q., Liu, Y.Z., Wu, H.X. and Zeng, Y.F. (2017), "Assessment of floor water inrush with vulnerability index method: application in Malan Coal Mine of Shanxi Province, China", *Q. J. Eng. Geol. Hydrogeol.*, **50**(2), 169-178. https://doi.org/10.1144/qjegh2016-105.
Wu, Q., Zhang, B., Zhao, W.D. and Liu, S.Q. (2013), "A new practical methodology of coal seam floor water burst evaluation: The comparison study among ANN, the weight of evidence, and the logistic-regression vulnerable index method based on GIS", *J. China Coal Soc.*, **38**(1), 21-26.
Xu, Z.G., Xian, M.T., Li, X.F., Zhou, W., Wang, J.M., Wang, Y.P. and Chai, J.R. (2021), "Risk assessment of water inrush in karst shallow tunnel with stable surface water supply: Case study", *Geomech. Eng.*, **25**(6), 495-508. https://doi.org/10.12989/gae.2021.25.6.495.
Zhang, B.L., Zhang, W., Shen, B.T., Gao, Y. and Liu, M.M. (2024), "Mechanisms of mining-induced inrush of pressurized water in the floor containing faults", *J. Theor. Appl. Mech.*, **62**(3). https://doi.org/10.1000/example_doi_placeholder.
Zhang, G.D., Xue, Y.G., Bai, C.H., Su, M.X., Zhang, K. and Tao, Y.F. (2021), "Risk assessment of floor water inrush in coal mines based on MFIM-TOPSIS variable weight model", *J. Cent. South Univ.*, **28**(8), 2360-2374. https://doi.org/10.1007/s11771-021-4825-2.
Zhang, N., Zhou, Y.F., Liu, J. and Wei, G.W. (2023), "VIKOR method for Pythagorean hesitant fuzzy multi-attribute decision-making based on regret theory", *Eng. Appl. Artif. Intell.*, **126**. https://doi.org/10.1016/j.engappai.2023.106857.
Zhang, S.C., Guo, W.J., Sun, W.B. and Yin, D.W. (2015), "Formation and evolution process of floor water inrush channel under high water pressure", *J. Shandong Univ. Sci. Technol. (Nat. Sci.)*, **34**(2), 25-29.
Zhang, Y.G. and Yang, L.N. (2021), "A novel dynamic predictive method of water inrush from coal floor based on gated recurrent unit model", *Nat. Hazards*, **105**(2), 2027-2043. https://doi.org/10.1007/s11069-020-04388-9.
Zhang, Y.J. and Li, F.M. (2022), "Prediction of water inrush from coal seam floors based on the effective barrier thickness", *Mine Water Environ.*, **41**(1), 168-175. https://doi.org/10.1007/s10230-022-00846-x.

GC